JOC The Journal of Organic Chemistry

Article

Cite This: J. Org. Chem. XXXX, XXX, XXX−XXX

pubs.acs.org/joc

Understanding the Alkylation of a Phenol by 1-(3-Chloropropyl)pyrrolidine: Evidence for the Intermediacy of an Azetidinium Ion

Ian W. Ashworth,*[,†] Lai C. Chan,[†] Brian G. Cox,[†] Ian M. McFarlane,[†] and Andrew R. Phillips[‡]

[†]Pharmaceutical Technology & Development, AstraZeneca, S41/11 Etherow, Silk Road Business Park, Macclesfield, SK10 2NA, United Kingdom

[‡]Early Product Development, Pharmaceutical Sciences, IMED Biotech Unit, AstraZeneca, Silk Road Business Park, Macclesfield, SK10 2NA, United Kingdom

Supporting Information

ABSTRACT: The final synthetic step in the synthesis of cediranib, AZD2171, **1**, is the alkylation of a phenol with an alkyl halide to generate an ether. Our need to understand and control the formation of synthetic impurities generated in this step of the synthesis led us to investigate the kinetics and mechanism of the alkylation of indolphenol, **2**, 4-[(4-fluoro-2-methyl-1*H*-indol-5-yl)oxy]-6-methoxyquinazolin-7-ol, by chloropyrrolidine, **3**, 1-(3-chloropropyl)pyrrolidine. Studies in 1-methyl-2-pyrrolidinone (NMP) established that the active alkylating agent is the azetidinium ion, **4**, 4-azoniaspiro[3.4]octane, formed via a slow intramolecular cyclization reaction of chloropyrrolidine, **3**. The azetidinium ion was isolated as its tetraphenylborate salt from water by heating **3** in the presence of aqueous potassium tetraphenyl borate, and its competence as an intermediate was demonstrated by its fast reaction with **2** to yield cediranib, **1**.

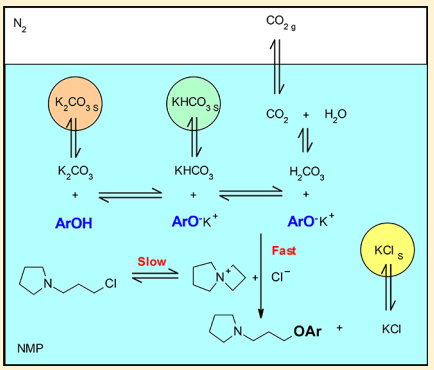

INTRODUCTION

AZD2171, cediranib, **1**, is an inhibitor of VEGF for the treatment of solid tumors.[1,2] The final synthetic step in the synthesis alkylates Indolphenol, **2**, with chloropyrrolidine (1-(3-chloropropyl)pyrrolidine), **3**, at elevated temperatures in NMP (1-methyl-2-pyrrolidinone) in the presence of K_2CO_3 (Scheme 1).[3] When scaling this process up, it was observed that the reaction time increased relative to the laboratory process and that elevated levels of an impurity were formed.

The formation of cediranib, **1**, by the alkylation of an aryloxide with an alkyl halide is an example of the classical Williamson ether synthesis.[4] As such, we expected the reaction to be a simple bimolecular substitution reaction,[5] but an examination of preliminary reaction profile data showed the reaction time to be independent of the reactant concentration. This behavior is consistent with first-order rather than the expected second-order kinetics.

In order to gain a better understanding of the alkylation we undertook a kinetic and mechanistic study of the reaction. As it was already known that deprotonation of **2** was required for the reaction to proceed we also investigated this in isolation from the alkylation. The results of these studies showed the active alkylating agent to be the Azetidinium ion, **4**, which was formed reversibly from **3** (Scheme 2). Under most conditions this was found to be the rate-limiting process in the alkylation reaction. The deprotonation of **2** by K_2CO_3 was found to be rapid relative to the overall reaction time. The base stoichiometry of 0.8 equiv, which had been selected based on lower levels of impurities in the isolated product, was identified as the likely cause of the slower reaction upon scale up.

RESULTS AND DISCUSSION

Preliminary Kinetic Studies. The simple alkylation of **2** to form cediranib, **1** (Scheme 1), would be expected to show second-order kinetics with a kinetic dependence upon the concentrations of both reactants. However, it was found that reactions carried out with initial reactant concentrations varying between 0.066 and 0.231 M occurred on very similar time scales (Figure 1). These reaction progress curves give a reasonable fit to first-order kinetics over most of the reaction. Additionally, little change was observed in the rate of reaction if indolphenol, **2**, was ionized, by stirring it for a period with K_2CO_3, prior to the addition of a solution of **3** in methyl tertiary butyl ether (MTBE) or if **3** was charged immediately after the K_2CO_3. These observations are inconsistent with a direct nucleophilic substitution between the anion of **2** and **3**, which would be expected to exhibit a kinetic dependence upon both reactant concentrations.

Qualitatively, these observations are consistent with the reactions shown in Scheme 3, in which product formation

Special Issue: Excellence in Industrial Organic Synthesis 2019

Received: September 24, 2018
Published: November 7, 2018

DOI: 10.1021/acs.joc.8b02458
J. Org. Chem. XXXX, XXX, XXX−XXX

Scheme 1. Alkylation To Form Cediranib, 1

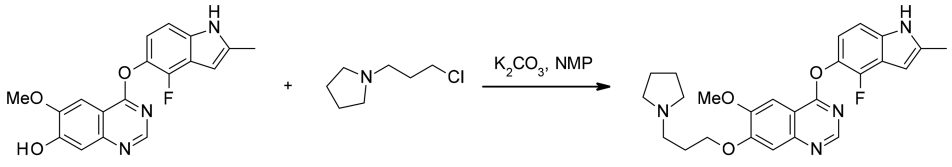

Indolphenol, **2** Chloropyrrolidine, **3** cediranib, **1**

Scheme 2. Formation of Azetidinium Ion, 4

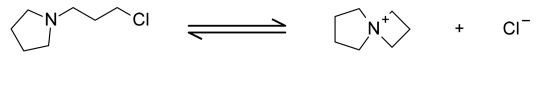

Chloropyrrolidine, **3** Azetidinium ion, **4**

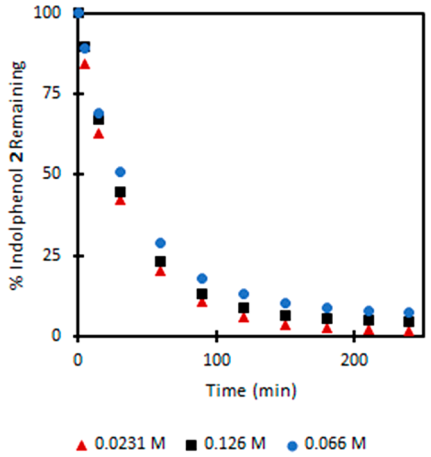

Figure 1. Reaction progress graphs for the alkylation of **2** by 1.05 equiv of **3** in 10:1 NMP/MTBE at 80 °C at different concentrations of **2**.

Scheme 3. Proposed Reaction Scheme for the Alkylation of Indolphenol, 2, by Azetidinium Ion, 4, Formed via the Cyclization of Chloropyrrolidine, 3

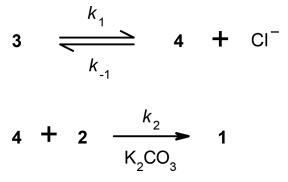

results from the alkylation of Indolphenol, **2**, by the azetidinium ion, **4**, formed by the slow, intramolecular cyclization of chloropyrrolidine, **3**.[6,7] Azetidinium ions, which are generally prepared by the alkylation of azetidines, are known to be effective alkylating agents.[8−11] This hypothesis was tested in our investigations of the alkylation reaction.

Treating the azetidinium ion, **4**, as a reactive intermediate and applying the steady-state approximation gives the below rate law (eq 1) for the formation of **1** and consumption of **2**. In deriving eq 1, it was assumed that $[Cl^-]$ is almost constant and it is included in k'_{-1} ($k'_{-1} = k_{-1}[Cl^-]$). This is due to the reaction generating KCl and $KHCO_3$ as stoichiometric byproducts, which precipitate from the reaction solvent.

$$\frac{d[\mathbf{1}]}{dt} = -\frac{d[\mathbf{2}]}{dt} = \frac{k_1 k_2 [\mathbf{3}][\mathbf{2}]}{k'_{-1} + k_2[\mathbf{2}]} \quad (1)$$

At high $[\mathbf{2}]$, $k_2[\mathbf{2}] \gg k'_{-1}$ and eq 1 simplifies to simple first-order kinetics, while, at low $[\mathbf{2}]$, $k'_{-1} \gg k_2[\mathbf{2}]$ meaning that eq 1 simplifies to second-order kinetics. Simultaneous fitting of the rate of loss of indolphenol, **2**, data to eq 1 (Figure 2) gave

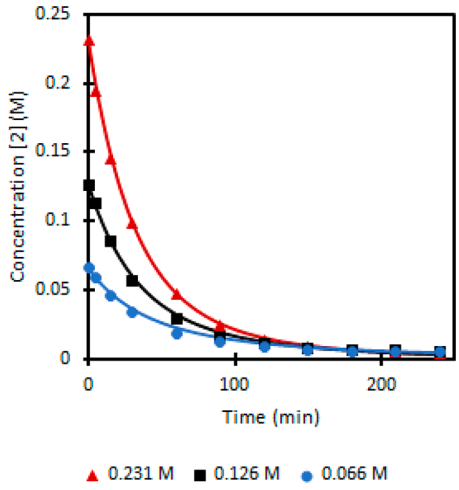

Figure 2. Best-fit curves for the fitting of eq 1 to the Indolphenol, **2**, loss curves generated at 80 °C in 10:1 NMP/MTBE with 1.05 equiv of **3**. $k_1 = 5.6 \times 10^{-4}$ s^{-1} and $k'_{-1}/k_2 = 0.034$ M.

values of k_1 of $5.6 \pm 0.3 \times 10^{-4}$ s^{-1} and k'_{-1}/k_2 0.034 ± 0.006 M.[12] The good agreement obtained between the model and the data provides strong support for the proposed mechanism (Scheme 3) involving reaction via the azetidinium ion, **4**. The value of 0.034 M obtained for k'_{-1}/k_2 represents the concentration of **2** at which the reaction changes from being predominantly first-order to being predominantly second-order. At high concentrations the rate-limiting step in the reaction is therefore the intramolecular cyclization of **3** to form the azetidinium ion, **4**.

In order to provide additional support to the proposed mechanism, the rates of formation and reaction of the azetidinium ion, **4**, were studied further in isolation from each other.

Deprotonation of Indolphenol. The use of K_2CO_3 as a heterogeneous base in the alkylation reaction to form **1** adds an additional complication, as indolphenol, **2**, deprotonation is required for reaction to occur. This raises the possibility that the rate of the deprotonation could control the rate of the alkylation reaction (Scheme 4). Studies of the deprotonation of 2-cyanophenol by K_2CO_3 in 1,1-dimethylformamide (DMF) have demonstrated that a similar heterogeneous deprotonation reaction is not instantaneous.[13]

An *in situ* attenuated total reflectance (ATR) UV−vis spectroscopic study of the deprotonation of **2** by K_2CO_3 at 80 °C in NMP was therefore undertaken. It was found that **2** could be observed at 325 nm, while the UV absorbance due to

DOI: 10.1021/acs.joc.8b02458
J. Org. Chem. XXXX, XXX, XXX−XXX

Scheme 4. Scheme for the Formation of Cediranib, 1, Including the Deprotonation of Indolphenol, 2 (ArOH), and Related Phase Equilibria

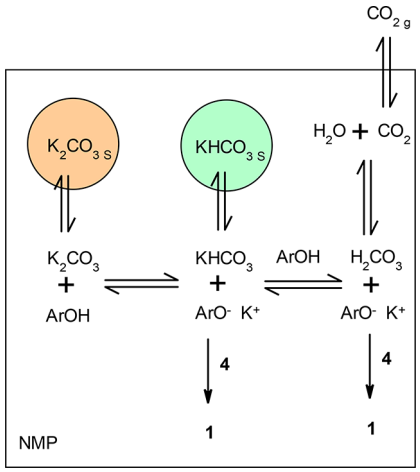

the phenoxide anion showed the expected bathochromic shift with absorptions at 270 and 353 nm.[14] As **2** had no absorbance at 353 nm this wavelength was used to monitor the deprotonation. A crude calibration curve of absorbance versus the solution concentration of the phenoxide was generated by adding known aliquots of potassium hydride to a solution of **2** in NMP.[15] Using this practical extinction coefficient it was possible to profile the deprotonation of **2** by K_2CO_3 at 80 °C under a range of process relevant conditions (Figure 3).

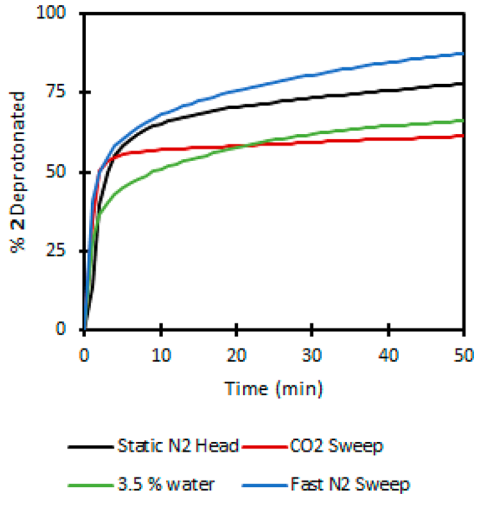

Figure 3. Deprotonation curves for **2** with 0.85 equiv of K_2CO_3 in NMP at 80 °C: effect of processing conditions.

Profiling the deprotonation of **2** under a static head of nitrogen provided a reasonable mimic of the manner in which the formation of **1** had been operated at scale. This experiment showed an initial rapid phase followed by a slower second phase (Figure 3) and achieved 90% deprotonation after 4 h. The initial rapid deprotonation was believed to be due to the K_2CO_3 present initially deprotonating **2**, while the subsequent slower deprotonation was believed to be due to $KHCO_3$ acting as a base to complete the deprotonation in agreement with the findings of Forryan et al.[13] The impact of using a sweep of nitrogen through the headspace of the deprotonation reaction was therefore investigated as a means of removing the CO_2 produced as a byproduct of the deprotonation by $KHCO_3$. This experiment gave a similar initially rapid deprotonation to the static head experiment, consistent with this portion of the curve being due to K_2CO_3. The subsequent $KHCO_3$ mediated phase of the deprotonation showed a significant acceleration consistent with the hypothesis that the removal of CO_2 from the deprotonation would promote the $KHCO_3$ mediated reaction. Further support was provided to this hypothesis by the performance of the deprotonation reaction when carried out under an atmosphere of CO_2. In this case the initial rapid K_2CO_3 mediated reaction gave a lower level of deprotonation than had been seen previously, followed by a very slow rate of ongoing deprotonation. The reduction in the initial anion yield was postulated to be due to CO_2 combining with water present in the NMP to generate a small quantity of carbonic acid, which partially neutralized the K_2CO_3 charged to the experiment. The addition of water (3.5% w/w) had an adverse effect upon the deprotonation of **2** and therefore the progress of the alkylation reaction, consistent with experimental observations during our development work.

Taken together the results of this study suggest that the likely explanation for the extension in the time taken to reach 95% conversion observed when scaling up the alkylation reaction was due to the substoichiometric K_2CO_3 charge. In the laboratory the loss of CO_2 from the reaction means that using $KHCO_3$ to complete the reaction is not problematic, whereas the operation of the reaction under a static head of nitrogen in a pilot plant slowed CO_2 disengagement leading to a long reaction tail. Operation of the reaction under a nitrogen sweep was therefore trialled in the laboratory and was demonstrated to be capable of achieving an acceptable reaction conversion with 0.6 equiv of K_2CO_3. This option was not pursued further, as it led to elevated levels of over-reaction products being formed.

Formation and Reaction of Azetidinium Ion, 4. Initial attempts to study the formation of **4** by heating a solution of chloropyrrolidine, **3**, in the reaction solvent (10:1 NMP/MTBE) gave little reaction by ^1H NMR. However, further NMR experiments demonstrated that **3** reacted in D_2O to give a single species, which was identified as the azetidinium ion, **4**. It was not possible to isolate **4**, prepared by stirring a suspension of **3** in water, as its chloride salt. Addition of either potassium tetraphenylborate or potassium hexafluorophosphate to this solution did give rise to isolable crystalline solids, which could be recrystallized from acetonitrile. The tetraphenylborate salt of **4** proved to be soluble in NMP and was used to study the kinetics of its reaction with indolphenol, **2** (see below).

(i) Kinetics of Azetidinium Ion, 4, Formation. The failure of the synthetic experiments to stoichiometrically generate **4** in the reaction solvent led us to hypothesize that the high activity of chloride in an aprotic solvent mixture suppressed the formation of **4**. Such reversibility in the formation of azetidinium ions has been observed in studies involving the cyclization of substituted 3-chloropropyl systems.[6] In the synthesis of cediranib, **1**, this is overcome by the presence of a high solution concentration of potassium in the form of the potassium salt of indolphenol, **2**, which removes the chloride from solution as KCl, leaving **4** in solution as its indolphenolate salt (Scheme 5). Addition of a soluble potassium salt, potassium tetraphenylborate, to a solution of chloropyrrolidine, **3**, in the reaction solvent, led to the

DOI: 10.1021/acs.joc.8b02458
J. Org. Chem. XXXX, XXX, XXX−XXX

Scheme 5. Scheme Illustrating the Coupling of the Precipitation of KCl with the Formation of Azetidinium Ion, 4, and Cediranib, 1

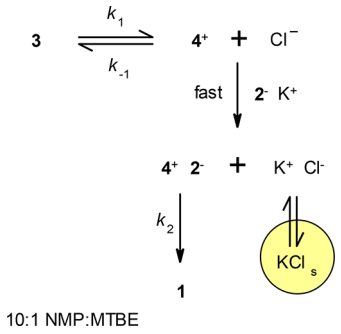

precipitation of KCl as the chloride as it was formed and made it possible to drive the reaction to completion.

This allowed us to undertake an *in situ* ^{1}H NMR study of the kinetics of the formation of **4** in 10:1 NMP/d_3-MTBE at 60, 70, and 77 °C. In addition to being able to see the loss of **3** and formation of **4**, we could also observe the slow formation of an additional species, which appeared to form from **4**. This was isolated as its tetraphenylborate salt and shown to be the chloropyrrolidine dimer, **5** (Scheme 6). The formation of the

Scheme 6. Kinetic and Mechanistic Scheme for the Formation of Azetidinium Ion, 4, and Dimer, 5, from Chloropyrrolidine, 3 (Including the ^{1}H NMR Resonances Used for Reaction Monitoring)

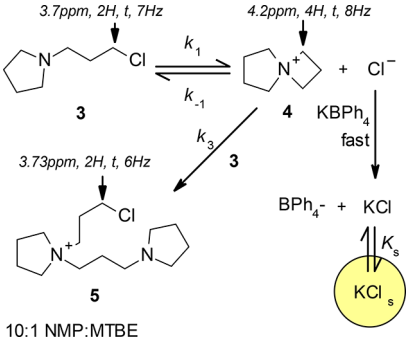

dimer, **5**, complicated the analysis of the ^{1}H NMR based kinetic data because its CH_2Cl resonance partially overlapped the CH_2Cl resonance of chloropyrrolidine, **3**. The application of mixed Gauss–Lorenz fitting[16] made it possible to deconvolute the overlapping triplets[17] and facilitated the generation of concentration versus time profiles (Figure 4) for the cyclization of **3**. The formation of the dimer, **5**, was not observed under normal preparative conditions due to the rapid reaction of **4** with **2** (see below).

The NMR derived concentration profiles were fitted[12] to a model (eqs 2–4) based on Scheme 6 to give the tabulated (Table 1) best-fit values of the rate constants.[18] A typical best-fit plot is shown in Figure 4.[19] In formulating eqs 2–4 it was assumed that the Cl^- concentration is held constant at the solubility of KCl.[20] A simple irreversible model, without the k'_{-1} term, was also investigated and found to give a worse fit to the data.

$$\frac{d[\mathbf{3}]}{dt} = -k_1[\mathbf{3}] + k'_{-1}[\mathbf{4}] - k_3[\mathbf{3}][\mathbf{4}] \quad (2)$$

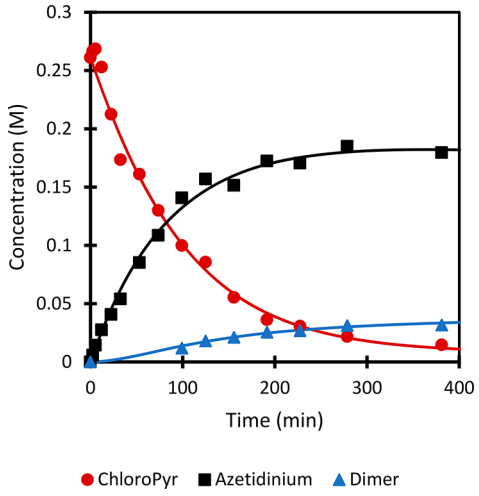

Figure 4. Best-fit plot for the cyclization of **3** (0.26 M) in 10:1 NMP/d_3-MTBE at 70 °C. The best-fit lines were calculated using eqs 2–4 with $k_1 = 1.48 \times 10^{-4}$ s^{-1}, $k'_{-1} = 8 \times 10^{-6}$ s^{-1}, and $k_3 = 1.96 \times 10^{-4}$ M^{-1} s^{-1}.

Table 1. Rate Constants for the Formation of Azetidinium Ion, 4, in 10:1 NMP/d_3-MTBE

temp (°C)	$10^4\ k_1$ (s^{-1})[a]	$10^4\ k'_{-1}$ (s^{-1})[a,b]	$10^4\ k_3$ (M^{-1} s^{-1})[a]
60	0.56 ± 0.02	0.03 ± 0.02	0.84 ± 0.07
70	1.48 ± 0.09	0.08 ± 0.07	1.96 ± 0.34
77	2.27 ± 0.11	0.13[c]	3.70 ± 0.41

[a]The uncertainties quoted for k_1, k'_{-1}, and k_3 are the 95% confidence limits derived from the fitting. [b]The reverse rate constant, k'_{-1}, was found to be strongly correlated with the other parameters in the model, as should be expected, and the confidence in the fitted values is therefore very low. [c]The uncertainty in the fitted value of k'_{-1} is greater than the fitted value meaning that the value is not statistically significant.

$$\frac{d[\mathbf{4}]}{dt} = k_1[\mathbf{3}] - k'_{-1}[\mathbf{4}] - k_3[\mathbf{3}][\mathbf{4}] \quad (3)$$

$$\frac{d[\mathbf{5}]}{dt} = k_3[\mathbf{3}][\mathbf{4}] \quad (4)$$

where $k'_{-1}=k_{-1}[Cl^-]$

The temperature dependence of the cyclization, k_1, and dimerization, k_3, rate constants follow the Arrhenius equation (Figure 5). The resultant activation energies are tabulated (Table 2) for each reaction alongside the enthalpy and entropy of activation obtained from Eyring plots.[21] The large negative entropy of activation obtained for the cyclization of **3** to yield **4** is rather surprising for a cyclization reaction to yield a small ring.[22] This is especially so when compared to the activation entropy of the bimolecular reaction to yield **5**, which is similar. A potential explanation may be found in the poor solvation of anions by dipolar aprotic solvents such as NMP, for which the free energy of transfer for chloride from water into NMP is 55.2 kJ mol^{-1} at 25 °C.[23] It is therefore plausible that the liberated chloride will either be associated with the product cation or stabilized by an interaction with another cation present in the reaction. Such associative interactions could offset the entropic gain to be expected from a unimolecular reaction that generates two product ions, leading to the unexpectedly large negative entropy of activation.

DOI: 10.1021/acs.joc.8b02458
J. Org. Chem. XXXX, XXX, XXX–XXX

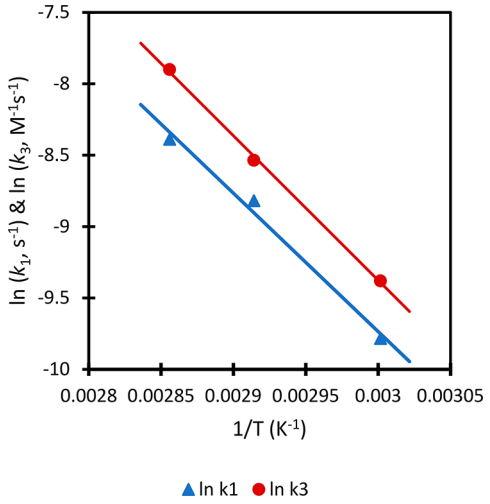

Figure 5. Arrhenius plot for the cyclization of **3** and its reaction with **4**.

A comparison of the first-order rate constant for the consumption of **3** in its reaction with **2**, 5.6×10^{-4} s^{-1} at 80 °C, with the predicted rate constant for the formation of **4** from **3** of 3.0×10^{-4} s^{-1} shows them to be similar. This is consistent with the proposed mechanistic hypothesis that the cyclization of **3** to generate **4** is the rate-limiting step in the formation of **1** at high concentrations (>0.04 M), which suggests that they should be comparable.

(ii) Kinetics of the Reaction between Indolphenol, 2, and Azetidinium Ion, 4. A comparison of the reaction between the azetidinium ion, **4**, as its tetraphenylborate salt and chloropyrrolidine, **3**, with indolphenol, **2**, potassium salt under similar conditions is shown (Figure 6). As expected, the reaction between the azetidinium ion, **4**, and **2** is rapid, achieving 50% conversion in less than 4 min, while the reaction with **3** is significantly slower, taking almost 100 min to reach the same point. This is consistent with the mechanistic hypothesis that the formation of **4** from **3** is the rate-limiting step in the formation of **1**.

Neither of the reactions (Figure 6) gave complete conversion of **3** or **4** to **1** due to the presence of a significant side reaction, which forms an isomeric byproduct. Comparison of the shapes of the profiles for the formation of **1** and the isomeric, *N*-alkylated, byproduct (Figure 7) from a reaction of **4** with **2** shows them to be similar, suggesting that the products are formed via competitive reactions with the same form of rate law (Scheme 7). Fitting of reaction profile data for the reaction of **4** as its tetraphenylborate salt with the potassium salt of **2** to a competitive second-order model (eqs 5–7) based on this hypothesis provides a good fit to the experimental data (Figure 8). The isomer is a result of the indolphenol, **2**, being an ambident nucleophile and capable of reacting via nitrogen as well as oxygen. No evidence was found for the opening of the pyrrolidine ring of the azetidinium ion, **4**, which is consistent with the 25 000-fold difference in reactivity between

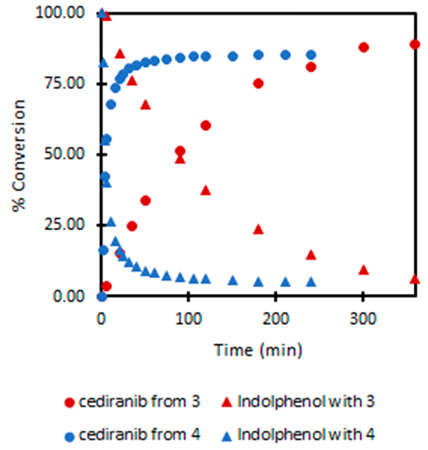

Figure 6. Reaction of indolphenol, **2**, with either **3** or **4** to form cediranib, **1**, in 10:1 NMP/MTBE at 70 °C. Chloropyrrolidine, **3**, reaction (circles): [**2**] = 0.233 M, [**3**] = 0.252 M. Azetidinium tetraphenylborate, **4**, reaction (triangles): [**2**] = 0.193 M, [**4**] = 0.197 M.

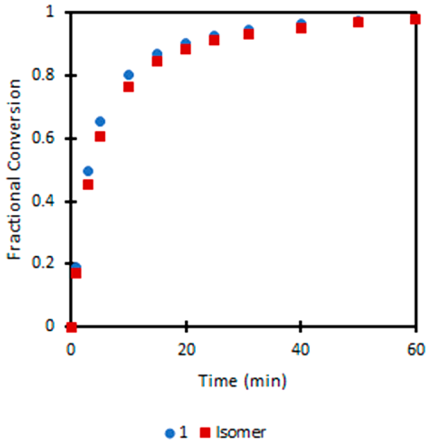

Figure 7. Comparison of the profiles for the formation of cediranib, **1**, and the isomeric byproduct in the reaction of the azetidinium ion, **4**, 0.18 M and indolphenol, **2**, potassium salt 0.19 M in 10:1 NMP/MTBE at 70 °C.

Scheme 7. Kinetic Scheme for the Formation of Cediranib, 1, and the Isomeric Byproduct from the Reaction of the Azetidinium Ion, 4, and Indolphenol, 2, Potassium Salt

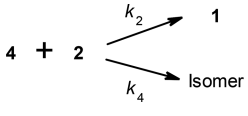

the 1,1-dimethyl azetidinium ion, **6**, and its pyrrolidinium analogue, **7**.[10]

The isomer formation is a known side reaction in the synthesis of cediranib, **1**, and represents a yield loss rather than a quality issue, as the isomer is purged in the crystallization of

Table 2. Summary of Activation Parameters for the Cyclization of 3 and Formation of 5[a]

reaction	constant	E_a (kJ mol^{-1})	A	$\Delta H^{\ddagger}$ (kJ mol^{-1})	$\Delta S^{\ddagger}$ (J K^{-1} mol^{-1})
cyclization of **3**	k_1 (s^{-1})	80 ± 15	2.5×10^8	78 ± 15	−94 ± 44
dimerization	k_3 (M^{-1} s^{-1})	84 ± 5	1.3×10^9	81 ± 5	−80 ± 15

[a]The uncertainties quoted are the 68% confidence bands from a simple linear regression analysis to determine the best-fit line.

DOI: 10.1021/acs.joc.8b02458
J. Org. Chem. XXXX, XXX, XXX−XXX

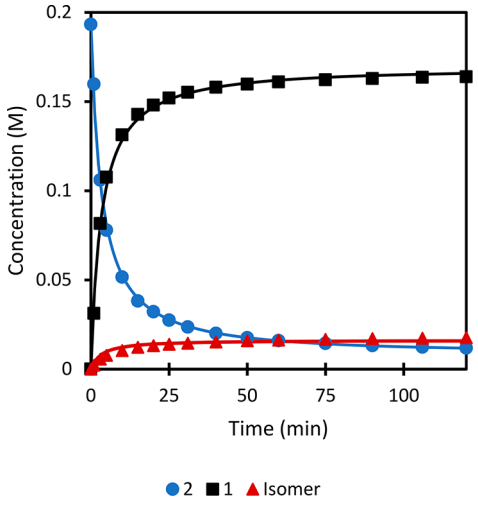

Figure 8. Best fit curves for the reaction of **4** BPh_4^- (0.18 M) with **2** K^+ (0.19 M) in 10:1 NMP/MTBE at 70 °C. The best-fit lines were calculated using eqs 5−7 with $k_2 = 2.40 \times 10^{-2}$ M^{-1} s^{-1} and $k_4 = 2.29 \times 10^{-3}$ M^{-1} s^{-1}.

cediranib, **1**. The competitive nature of the isomer formation means that changes to the reaction stoichiometry, order, or mode of reactant addition will not modify the selectivity of the reaction for **1** over its isomer.

$$-\frac{d[\mathbf{4}]}{dt} = -\frac{d[\mathbf{2}]}{dt} = k_2[\mathbf{2}][\mathbf{4}] + k_4[\mathbf{2}][\mathbf{4}] \quad (5)$$

$$\frac{d[\mathbf{1}]}{dt} = k_2[\mathbf{2}][\mathbf{4}] \quad (6)$$

$$\frac{d[\text{Isomer}]}{dt} = k_4[\mathbf{2}][\mathbf{4}] \quad (7)$$

Attempts to simultaneously fit reaction progress data from reactions at two different process concentrations to a model based on eqs 5−7 failed. Individual fitting of both sets of experimental data was successful to give the tabulated best-fit rate constants (Table 3).[12,24] These clearly show the reaction

Table 3. Concentration Dependence of Rate Constants for the Formation of Cediranib, 1, from Azetidinium, 2, Tetraphenylborate and Indolphenol, 2, Potassium Salt in 10:1 NMP/MTBE at 70 °C

[2K] (M)	[4BPh_4] (M)	10^2 k_2 (M^{-1} s^{-1})	10^2 k_4 (M^{-1} s^{-1})
0.193	0.183	2.40 ± 0.12	0.23 ± 0.02
0.103	0.101	6.10 ± 0.13	0.33 ± 0.02

to be significantly faster under more dilute conditions. A likely explanation of this behavior is that strong ion pairing is occurring between the anion of indolphenol, **2**, and K^+ as has been observed previously in kinetic studies of a range of phenoxide ions with butyl bromide in the presence of alkali metal cations.[25] The formation of an ion pair leads to a portion of the phenoxide being in a less reactive or unreactive complex and therefore reduces the rate of reaction as the concentration of the metal cation is increased. This behavior was not investigated further, as it was of limited relevance to the conditions used to form cediranib, **1**, where the K^+ concentration is kept low by the precipitation of KCl (Scheme 5) and the rate-limiting step is the formation of the azetidinium ion, **4**.

Comparing the rate constant for the formation of dimer **5** at 70 °C (2.29×10^{-4} M^{-1} s^{-1}) with the rate constant for the reaction of azetidinium ion **4** with the potassium salt of indolphenol, **2** (2.4×10^{-2} M^{-1} s^{-1}), shows that product formation should outcompete dimer formation. However, this will not be the case if the deprotonation of indolphenol, **2**, is inefficient. This may in part explain the slow reaction observed when the process was scaled-up.

In summary, the first-order kinetics observed during investigations of the alkylation of a phenoxide by an alkyl chloride to synthesize cediranib have been rationalized in terms of the alkyl chloride undergoing a slow intramolecular cyclization reaction to generate an azetidinium ion, which is the active alkylating species in the etherification. The kinetics of the cyclization of the alkyl chloride were studied independently by ^{1}H NMR spectroscopy and shown to be consistent with this hypothesis. Our isolation of the azetidinium ion as its tetraphenylborate salt enabled us to demonstrate that the azetidinium ion reacts rapidly with the phenoxide in a reaction that exhibited second-order kinetics, which agrees with our mechanistic proposal. Additional studies of the heterogeneous deprotonation of the phenol by K_2CO_3 confirmed that significant deprotonation occurs relatively rapidly under the synthetic conditions. However, the process uses substoichiometric K_2CO_3, which means that a portion of the deprotonation is carried out by $KHCO_3$, and therefore generates CO_2 as a byproduct. Failure to disengage this CO_2 from the reaction mass has been demonstrated to be capable of stalling the deprotonation. It is also a potential cause of the extended reaction times observed at plant scale when the process was scaled-up. This was mitigated by increasing the K_2CO_3 charge used in the process, so that the deprotonation by $KHCO_3$ was a less significant contributor to the progress of the reaction. In the event of the deprotonation reaction stalling, the azetidinium ion will continue to be generated whereupon it has the potential to dimerize or react through other manifolds.

EXPERIMENTAL SECTION

General Information. Except where stated, all reagents were purchased from commercial sources and used without further purification. Unless stated to the contrary, reactions were heated by means of circulating oil baths operating in batch temperature mode. ^{1}H NMR and ^{13}C NMR spectra were recorded on a Bruker DRX spectrometer operating at 499.9 and 125.7 MHz or on a Bruker DPX spectrometer operating at 400 and 101 MHz respectively. All spectral data were collected at 300 K unless it is stated to the contrary. Chemical shifts (δ) are quoted in parts per million (ppm) relative to TMS. Coupling constants (J) are reported in hertz (Hz) to the nearest 0.1 Hz. The multiplicity abbreviations used are s, singlet; d, doublet; and m, multiplet. Signal assignments were achieved by analysis of HSQC-DEPT, COSY, and HMBC experiments. Mass spectra (high resolution) were obtained using electrospray ionization in positive ion mode (ESI) on a Bruker Daltonics MicrO-TOFQ spectrometer. Strengths quoted for materials were determined by HPLC against an external standard of the appropriate compound or by ^{1}H NMR, at least in duplicate, against an internal standard of benzyl benzoate. HPLC analyses were undertaken using the below method on an Agilent 1100 series instrument with a quaternary pump and variable wavelength diode detector.[26]

Sample Kinetic Procedures. *Preliminary Kinetic Studies.* Indolphenol, **2**, NMP solvate (19.42 g @99.8% w/w, 44.3 mmol), and K_2CO_3 (6.9 g, 35.4 mmol) were charged to a 250 mL jacketed

DOI: 10.1021/acs.joc.8b02458
J. Org. Chem. XXXX, XXX, XXX−XXX

reactor fitted with a retreat curve agitator, thermocouple, condenser, and N_2 bubbler. NMP (152 mL) was charged, and the agitator was started (250 rpm). The slurry was heated to 80 °C and then held at 80 °C for 1 h before chloropyrrolidine, **3**, in MTBE (15.75 g @ 43.6% w/w, 46.5 mmol) was added and rinsed in with MTBE (3.6 mL). The reaction mass was stirred at 80 °C for 4 h sampling periodically. Sample preparation procedure: 30−40 μL of reaction mass added into 25 mL volumetric flask and make up to the line with HPLC sample diluent.

Chloropyrrolidine Cyclization Kinetics by ^{1}H NMR. $KBPh_4$ (391 mg @ 97% w/w, 1.06 mmol) was dissolved in NMP (2.17 mL). Chloropyrrolidine, **3**, (105 mg, 0.71 mmol), which had been evaporated to an oil at room temperature, was dissolved in d_3-MTBE (210 μL). The two solutions were mixed thoroughly and transferred to a 5 mm NMR tube. The tube was placed in a 400 MHz NMR spectrometer operating at a probe temperature of 350 K, and ^{1}H NMR spectra were recorded periodically for 7 h. A blank sample without the chloropyrrolidine was used to check the relaxation times to ensure that the delay between pulses was sufficient.

*Kinetics of Azetidinium, **4**, Tetraphenylborate with Indolphenol, **2**, Potassium Salt.* Indolphenol, **2** (4.13 g at 72.6%, 7.95 mmol), potassium salt was charged to a dry 80 mL multinecked jacketed vessel containing a magnetic stirrer flea followed by NMP (29.9 mL). The slurry was heated to 70 °C with stirring under N_2 to give a clear red solution. Azetidinium tetraphenylborate, **4** (3.58 g @ 97.2% w/w, 8.06 mmol), was charged and rinsed in with MTBE (3.0 mL), and the reaction mass was stirred at 70 °C for 6 h with periodic sampling. Sample preparation procedure: 40 μL of reaction mass added into a 25 mL volumetric flask and make up to the line with HPLC sample diluent.

Sample Indolphenol Deprotonation Procedure. A 500 mL jacketed reactor was set up with a retreat curve agitator, thermocouple, condenser, and N_2 bubbler. A 12.7 mm titanium ATR-UV vis probe with a sapphire ATR crystal was positioned in the vessel above the agitator. The probe was connected to a Zeiss UV−visible spectrometer (running Aspect Plus V1.52) via 3 m fiber optic cables. NMP (150 mL) was charged to the vessel and heated to 80 °C with stirring. Once the temperature was stable, an NMP background spectrum was recorded. Indolphenol, **2** (9.7 g @ 99% w/w, 22.2 mmol), NMP solvate was charged and washed with NMP (10 mL) and the mixture was stirred at 80 °C for 10 min. Data collection was started, collecting spectra from 245 to 510 nm every minute for the first hour and then every 2 min for the next 2 h. After 10 min, K_2CO_3 (2.6 g, 18.8 mmol) was charged and the reaction was stirred for 3 h under a static head of N_2.

Synthetic Procedures. *Indolphenol, 4-[(4-Fluoro-2-methyl-1H-indol-5-yl)oxy]-6-methoxyquinazolin-7-ol, **2** as Its NMP Solvate.* 3% Palladium on carbon (1.0 g of 60% water wet catalyst, 0.17 mmol Pd) was charged to a 1 L jacketed hydrogenation vessel fitted with a six blade Rushton turbine agitator, and the vessel was purged three times with N_2. 7-(Benzyloxy)-4-[(4-fluoro-2-methyl-1*H*-indol-5-yl)-oxy]-6-methoxyquinazoline[3] (76.1 g @ 98.6% w/w, 0.175 mol) was dissolved in 1-methyl-2-pyrrolidinone, NMP (407 mL), and the solution was transferred into the hydrogenator followed by NMP (38 mL) as a wash. The hydrogenator was purged three times with N_2. The contents of the hydrogenator were heated to 45 °C with stirring. Once the temperature was stable at 45 °C, the agitator was stopped, and the vessel was purged 3 times with hydrogen before pressurizing to 3 barg with hydrogen. Agitation was restarted, the vessel contents were maintained at 45 °C, and the hydrogen uptake was monitored at constant pressure. After 3 h, the hydrogen uptake had leveled off at 4.14 L (97% of theory). The hydrogen delivery and agitator were stopped, and the vessel was purged three times with N_2. The batch was discharged from the vessel and filtered through a double layer of Pall filter paper to remove the catalyst, and the vessel was rinsed with NMP (60 mL). These rinsings were used to wash the catalyst and combined with the product solution. A brown solution of **2** in NMP (564 g @ 10% w/w, 96% yield) was obtained.

At plant scale this solution was telescoped directly into the alkylation reaction to form **1**. In the laboratory it was customary to carry out the hydrogenation on a scale that meant it could be used to supply a number of alkylation reactions.

A solution of indolphenol, **2**, in NMP (400 g @ 10% w/w, 0.118 mol) was charged to a 1 L jacketed vessel fitted with a retreat curve agitator, thermocouple, condenser, and N_2 bubbler. Agitation was started (350 rpm), and the contents of the vessel were thermostated to 20 °C. Acetonitrile (400 mL) was charged over 30 min via a pressure equalizing dropping funnel, and the solution stirred at 20 °C for 4 h (seed may optionally be added after the acetonitrile). The resultant pale buff slurry was heated to 46 °C over 30 min, held at 46 °C for a further 30 min, cooled to 0 °C over 4 h, and finally cooled to −20 °C over 3 h. The solid product was isolated on a split Buchner funnel under reduced pressure after stirring for 1 h at −20 °C. An acetonitrile displacement wash (80 mL) was applied to the filter cake, and the damp product was dried overnight in a vacuum oven at 45 °C to give indolphenol **2** NMP solvate (36.39 g @ 99.8% w/w, 70% yield) as a white solid; ^{1}H NMR (400 MHz, DMSO-*d6*) δ = 11.11 (br s, 1H), 10.38 (br s, 1H), 8.41 (s, 1H), 7.61 (s, 1H), 7.24 (s, 1H), 7.19−7.09 (m, 1H), 7.01−6.90 (m, 1H), 6.26−6.18 (m, 1H), 4.00 (s, 3H), 2.41 (s, 3H); ^{13}C{^{1}H} NMR (101 MHz, DMSO-*d6*) δ = 164.4, 154.2, 151.8, 149.6, 148.6, 145.5 (d, J = 245.3 Hz), 137.1, 136.0 (d, J = 10.9 Hz), 130.6 (d, J = 11.3 Hz), 117.7 (d, J = 19.2 Hz), 115.3, 109.6, 108.6, 106.26 (d, J = 3.4 Hz), 101.2, 94.8, 55.8, 12.8; HRMS (ESI/Q-TOF) m/z: $[M + H]^+$ calcd for $C_{18}H_{15}FN_3O_3$ 340.1092; found 340.1094.

Chloropyrrolidine, 1-(3-chloropropyl)pyrrolidine,[27] **3**, as a solution in MTBE. Chloro-pyrrolidine, **3**, oxalate (58.1 g, 0.244 mol) and deionized water (100 mL) were charged to a 500 mL jacketed reaction vessel fitted with a retreat curve agitator, pressure equalizing dropping funnel, thermocouple, condenser, and N_2 bubbler. The mixture was agitated (600 rpm), and methyl *tert*-butyl ether (MTBE) (50 mL) was charged. The resultant biphasic solution was cooled to 10 °C, and 50% w/w KOH solution (60.8 g, 0.531 mol) was added over 1 h keeping the temperature below 20 °C. After the mixture was warmed to 20 °C, the agitator was stopped, and the phases were separated. The lower pale yellow aqueous phase was returned to the vessel, MTBE (50 mL) was added, and the mixture was agitated for 15 min at 20 °C. The agitator was stopped, the phases were separated, and the combined organic phases (∼130 mL) were returned to the vessel. A 30% w/w solution of KCl (25 mL) was charged, and the mixture was agitated for 30 min at 20 °C. The phases were allowed to separate, and the upper phase was retained. This gave chloropyrrolidine, **3** (108 g @ 33% w/w, 0.241 mol), as a solution in MTBE.

Free basing of **3** was usually carried out on a scale sufficient to supply a number of experiments, and the resulting solution of **3** in MTBE was stored in the freezer. We also used a similar procedure with less base to free base the HCl salt of **3**.

*AZD2171, Cediranib, 4-[(4-Fluoro-2-methyl-1H-indol-5-yl)oxy]-6-methoxy-7-[3-(pyrrolidin-1-yl)propoxy]quinazoline, **1**.* K_2CO_3 (2.6 g, 18.6 mmol) was charged to a 250 mL jacketed reaction vessel fitted with a retreat curve agitator, thermocouple, condenser, and N_2 bubbler. The vessel was thoroughly purged with N_2, and indolphenol, **1** (78.9 g @ 10% w/w, 23.2 mmol), in NMP was charged followed by an NMP (7.9 mL) wash. Chloropyrrolidine, **3** (10.9 g @ 33% w/w, 24.4 mmol), in MTBE was charged followed by MTBE (1 mL) as a wash. The agitator was started (300 rpm), the vessel was heated to 72 °C over 30 min, and the contents stirred at 72 °C under N_2 for 21 h. Water (87 mL) was charged maintaining the temperature above 60 °C, and the slurry was allowed to self-cool to ambient with stirring. The solid product was isolated by filtration under reduced pressure after 2 h, and the filter cake was washed with a mixture of NMP (7.2 mL) and water (7.2 mL) followed by three water washes (14.4 mL each). The product was dried in a vacuum oven to give cediranib, **1** (9.07 g @ 99.5% w/w, 86% yield), a white solid; ^{1}H NMR (400 MHz, DMSO-d_6) δ = 11.32 (br s, 1H), 8.49 (s, 1H), 7.59 (s, 1H), 7.36 (s, 1H), 7.15 (dd, J = 8.5, 0.4 Hz, 1H), 6.98 (dd, J = 8.5, 7.4 Hz, 1H), 6.24−6.21 (m, 1H), 4.23 (t, J = 6.5 Hz, 2H), 3.98 (s, 3H), 2.55 (t, J = 7.2 Hz, 2H), 2.47−2.42 (m, 4H), 2.42−2.38 (m, 3H), 2.03−1.92 (m, 2H), 1.72−1.64 (m, 4H); ^{13}C{^{1}H} NMR (101 MHz, DMSO-d_6) δ = 164.6, 155.1, 152.3, 150.2,

DOI: 10.1021/acs.joc.8b02458
J. Org. Chem. XXXX, XXX, XXX−XXX

148.8, 145.7 (d, J = 245.4 Hz, 1C), 137.5, 136.3 (d, J = 11.3 Hz, 1C), 130.7 (d, J = 11.3 Hz, 1C), 117.9 (d, J = 18.8 Hz, 1C), 115.5, 109.2, 107.3, 106.7 (d, J = 3.4 Hz, 1C), 100.7, 95.1, 67.1, 56.0, 53.6 (s, 2C), 52.1, 27.9, 23.1 (s, 2C), 13.3; HRMS (ESI/Q-TOF) m/z: $[M + H]^+$ calcd for $C_{25}H_{28}FN_4O_3$ 451.2140; found 451.2131.

*Azetidinium Ion, 4-Azoniaspiro[3.4]octane Tetraphenylborate, **4**.* Chloropyrrolidine, **3** (20 g, 0.135 mol), in toluene (200 mL) was charged to a 500 mL jacketed reaction vessel fitted with a retreat curve agitator, thermocouple, condenser, and N_2 bubbler and heated at 80 °C for 3 h. Water (25 mL) was added to the mixture over 30 min keeping the reaction temperature between 70 and 85 °C. The mixture was then allowed to settle for 15 min, and the lower aqueous phase separated off. The organic phase was washed with water (25 mL) at 80 °C, and the lower aqueous phases were combined. The aqueous solution (containing the azetidinium chloride salt) was then added to a solution of sodium tetraphenylborate (46.6 g @ 99.5%w/w, 0.135 mol) in acetone (180 mL) over 15 min at 20 °C. The white precipitate was filtered, washed with water (3 × 100 mL), and then dried in a vacuum oven at 45 °C for 48 h to give azetidinium tetraphenylborate, **4** (52.4 g @ 97% w/w, 87% yield), a white crystalline solid; mp 233−234 °C; ^{1}H NMR (400 MHz, DMSO-*d*6) δ = 7.32−7.06 (m, 8H), 7.04−6.86 (m, 8H), 6.86−6.68 (m, 4H), 4.34−4.04 (m, 4H), 3.58−3.42 (m, 4H), 2.46−2.33 (m, 2H), 2.01−1.80 (m, 4H); ^{13}C{^{1}H} NMR (101 MHz, DMSO-*d*6) δ = 164.1−162.5 (m, 4C), 135.6−135.3 (m, 8C), 125.4−125.1 (m, 8C), 121.5 (s, 4C), 62.1−61.9 (m, 4C), 20.7 (s, 2C), 14.1; HRMS (ESI/Q-TOF) m/z: $[M]^+$ calcd for $C_7H_{14}N$ 112.1121; found 112.1128.

*Dimer, 1-(3-Chloropropyl)-1-[3-(pyrrolidin-1-yl)propyl]-pyrrolidin-1-ium Tetraphenylborate, **5**.* Chloropyrrolidine, **3** (74.8 mg @ 99% w/w, 0.5 mmol), and azetidinium tetraphenylborate, **4** (222 mg @ 97% w/w, 0.5 mmol), were dissolved in dry acetonitrile (3.4 mL) in a 25 mL multinecked flask containing a magnetic stirrer flea and fitted with a thermocouple, condenser, and N_2 bubbler. The solution was heated to 80 °C in an aluminum block on a hot plate stirrer and stirred at 80 °C for 8 h. Upon cooling a white precipitate formed, which was isolated by filtration under reduced pressure and washed with cold acetonitrile (0.5 mL). The wet product was dried overnight in a vacuum oven at 45 °C to give dimer tetraphenylborate, **5** (83 mg @ 94%, 27% yield); ^{1}H NMR (400 MHz, acetonitrile-*d*3) δ = 7.40−7.18 (m, 8H), 7.05−7.00 (m, 8H), 6.93−6.80 (m, 4H), 3.64−3.57 (m, 2H), 3.34−3.29 (m, 4H), 3.26−3.20 (m, 2H), 3.22−3.16 (m, 2H), 2.52−2.48 (m, 4H), 2.50−2.47 (m, 2H), 2.14−2.09 (m, 2H), 2.09−2.03 (m, 4H), 1.85−1.77 (m, 2H), 1.79−1.72 (m, 4H); ^{13}C{^{1}H} NMR (126 MHz, acetonitrile-*d*3) δ = 165.5−164.3 (m, 4C), 136.8 (s, 8C), 127.0−126.3 (m, 8C), 122.9 (s, 4C), 64.4−64.3 (m, 2C), 59.5−59.4 (m, 1C), 58.3−58.1 (m, 1C), 54.8 (s, 2C), 53.1, 42.5, 27.1, 24.4 (s, 2C), 23.4, 22.5 (s, 2C); HRMS (ESI/Q-TOF) m/z: $[M]^+$ calcd for $C_{14}H_{28}ClN_2$ 259.1936; found 259.1931.

■ ASSOCIATED CONTENT

Supporting Information

The Supporting Information is available free of charge on the ACS Publications website at DOI: 10.1021/acs.joc.8b02458.

Repetitive scanning UV−vis plot of the deprotonation of **2**; plot of absorbance at 353 nm versus phenoxide concentration for the deprotonation of **2**; best-fit plots for the cyclization of **3** at 60 and 77 °C; Micromath Scientist models and notes on the kinetic fitting; extension to eqs 2−4 to include the equilibrium solubility of KCl; Eyring plots for the cyclization of **3** (k_1) and its reaction with **4** (k_3); best-fit plot for the reaction of **4** (0.10 M) with the potassium salt of **2** (0.10 M) at 70 °C; HPLC method for cediranib **1** and indolphenol **2**; ^{1}H and ^{13}C NMR spectra of cediranib, **1**, indolphenol (NMP solvate), **2**, azetidinium tetraphenylborate, **4**, and dimer tetraphenylborate, **5** (PDF)

■ AUTHOR INFORMATION

Corresponding Author

*E-mail: ian.ashworth@astrazeneca.com.

ORCID

Ian W. Ashworth: 0000-0001-7210-3875

Notes

The authors declare no competing financial interest.

■ ACKNOWLEDGMENTS

Firstly, the authors would like to acknowledge the significant intellectual and experimental contribution made to this work by Dr. E. A. Arnott. The authors also thank Dr. S. Coombes and Dr. A. Bristow for assistance with NMR and mass spectrometric characterization, respectively. Mrs. E. Brazier, Mr. M. Senior, and Mr. M. Evans provided materials to support this work, whilst Dr. M. F. Jones provided significant encouragement and support. Finally, the authors acknowledge the support of AstraZeneca in carrying out this work.

■ REFERENCES

(1) Hennequin, L. F. A.; Ple, P.; Stokes, E. S. E.; McKerrecher, D. Preparation of quinazoline derivatives as angiogenesis inhibitors; WO2000047212A1 [139:164806].

(2) Wedge, S. R.; Kendrew, J.; Hennequin, L. F.; Valentine, P. J.; Barry, S. T.; Brave, S. R.; Smith, N. R.; Dukes, M.; Curwen, J. O.; Chester, R.; Jackson, J. A.; Boffey, S. J.; Kilburn, L. L.; Barnett, S.; Richmond, G. H. P.; Wadsworth, P. F.; Walker, M.; Bigley, A. L.; Taylor, S. T.; Cooper, L.; Beck, S.; Jurgensmeier, J. M.; Ogilvie, D. J. AZD2171: a highly potent, orally bioavailable, vascular endothelial growth factor receptor-2 tyrosine kinase inhibitor for the treatment of cancer. *Cancer Res.* **2005**, *65*, 4389−4400.

(3) Arnott, E. A.; Crosby, J.; Evans, M. C.; Ford, J. G.; Jones, M. F.; Leslie, K. W.; McFarlane, I. M.; Sependa, G. J. Process for preparation of 4-fluoro-2-methyl-1*H*-indol-5-ol from fluorohalonitrobenzenes and acetoacetate esters; WO2008053221A2, [148:517536].

(4) (a) Williamson, A. 'Theory of etherification'. *Philos. Mag.* **1850**, *37* (251), 350−356. (b) Feuer, H.; Hooz, J. In *The Chemistry of the Ether Linkage*; Patai, S., Ed.; Wiley: New York, 1967; pp 448−450 and 460−468.

(5) Isaacs, N. S. *Physical organic chemistry*, 2nd ed.; Pearson Education: Harlow, England, 1995; pp 418−433.

(6) Gaertner, V. R. 'Ring-opening alkylations of 1,1-dialkyl-3-substituted azetidinium cations. Substituent entropy-controlled strained ring-chain equilibria'. *J. Org. Chem.* **1968**, *33*, 523−530.

(7) Salomon, G. 'Kinetics of ring-formation and polymerization in solution'. *Trans. Faraday Soc.* **1936**, *32*, 153−175 and references therein .

(8) Couty, F.; Evano, G. 'Azetidines: New tools for the synthesis of nitrogen heterocycles'. *Synlett* **2009**, *2009*, 3053−3064.

(9) Couty, F.; David, O.; Durrat, F.; Evano, G.; Lakhdar, S.; Marrot, J.; Vargas-Sanchezlal, M. 'Nucleophilic ring-opening of azetidinium ions: insights into regioselectivity'. *Eur. J. Org. Chem.* **2006**, *2006*, 3479−3490.

(10) Cospito, G.; Illuminati, G.; Lillocci, C.; Petride, H. 'Ring-opening reactions. 3. Mechanistic path vs. ring-strain control in elimination and substitution reactions of 1,1-dimethyl cyclic ammonium ions and their α,α'-dimethyl-substituted derivatives'. *J. Org. Chem.* **1981**, *46*, 2944−2947.

(11) Illuminati, G.; Lillocci, C. 'Ring-opening reactions.1. Decomposition of some quaternary ammonium ions with sodium methoxide in methanol'. *J. Org. Chem.* **1977**, *42*, 2201−2203.

(12) Fitted using Micromath Scientist V3, www.micromath.com. The quoted errors are the 95% confidence intervals arising from the fitting. A copy of the model used in text format may be found in the Supporting Information (SI).

DOI: 10.1021/acs.joc.8b02458
J. Org. Chem. XXXX, XXX, XXX−XXX

(13) Forryan, C. L.; Klymenko, O. V.; Brennan, C. M.; Compton, R. G. 'Heterogeneous kinetics of the dissolution of an inorganic salt, potassium carbonate, in an organic solvent, dimethylformamide'. *J. Phys. Chem. B* **2005**, *109*, 8263−8269.
(14) A repetitive scan plot of the spectra during the deprotonation reaction may be found in SI Figure S1.
(15) A plot of absorbance at 353 nm versus potassium indolphenolate, **2**, concentration may be found in SI Figure S2.
(16) Using the peak fitting algorithm within ACD/Spectrus Processor, Advanced Chemistry Development Inc., Toronto, Canada, www.acdlabs.com.
(17) While the $-CH_2Cl$ resonances of **3** and **5** are triplets, the N^+-CH_2- signals of **4** are a pseudotriplet due to nonequivalence of the protons on the adjacent CH_2 group.
(18) The correlation between the rate constants observed in fitting the model is a mathematical consequence of fitting all the constants in the model. This issue was avoided when fitting eq 1 by fitting the ratio k'_{-1}/k_2 rather than k'_{-1} and k_2. However, in this case we were interested in obtaining an estimate of the rate constant of the dimerization reaction from the limited data available. An independent measurement of the equilibrium constant ($K = k_1/k'_{-1}$) for the cyclization of **3** would resolve the issue, as would simultaneous fitting of multiple sets of profile data collected at different reactant concentrations.
(19) Best-fit plots for the reaction at 60 and 77 °C may be found in SI Figures S3 and S4, respectively.
(20) This is a simplification that ignores the fact that KCl has a solubility product, $K_s = [K^+][Cl^-]$. A correct treatment may be found in the SI. This was unsuitable for application with the available experimental data, as it introduced an extra parameter to be fitted in a model that was already exhibiting significant correlation between the parameters in the fitting.
(21) An Eyring plot for both k_1 and k_3 may be found in SI Figure S5.
(22) Illuminati, G.; Mandolini, L. 'Ring closure reactions of bifunctional chain molecules'. *Acc. Chem. Res.* **1981**, *14*, 95−102.
(23) Cox, B. G. *Acids and Bases. Solvent Effects on Acid-Base Strength*; Oxford University Press: Oxford, 2013, pp 27−34 and references therein.
(24) A best-fit plot for the reaction of 0.10 M **4**BPh_4 with 0.11 M **2**K in 10:1 NMP/MTBE at 70 °C may be found in SI Figure S6.
(25) Illuminati, G.; Mandolini, L.; Masci, B. 'Template effects. 4. Ion pairing of aryloxide ions with alkali cations in 99% dimethyl sulfoxide: influence on the rate of formation of benzo-18-crown-6 and of other Williamson-type reactions'. *J. Am. Chem. Soc.* **1983**, *105*, 555−563.
(26) Full details of the HPLC method used and typical retention times may be found in the SI.
(27) (a) Gray, A. P.; Archer, W. L.; Schlieper, D. C.; Spinner, E. E.; Cavallito, C. J. 'Bis-ammonium salts. Unsymmetrical derivatives of some isoquinolines and related heterocyclic bases'. *J. Am. Chem. Soc.* **1955**, *77*, 3536−3541. (b) Yale, H. L. '3-Chloro-10-dialkylaminoalkylphenothiazines'. *J. Am. Chem. Soc.* **1955**, *77*, 2270−2272.

DOI: 10.1021/acs.joc.8b02458
J. Org. Chem. XXXX, XXX, XXX−XXX